Advances in Science and Technology Research Journal

Advances in Science and Technology Research Journal 2022, 16(5), 28–39
https://doi.org/10.12913/22998624/153045
ISSN 2299-8624, License CC-BY 4.0

Received: 2022.07.01
Accepted: 2022.10.17
Published: 2022.11.01

Construction and Verification for Metrological Properties of the Prototype Magnetic Head for Nondestructive Testing of Lift Guide Rail Wear under Test Conditions

Tomasz Krakowski[1], Hubert Ruta[1], Paweł Lonkwic[2*], Arkadiusz Tofil[2]

[1] Faculty of Mechanical Engineering and Robotics, AGH University of Science and Technology, aleja Adama Mickiewicza 30, Kraków 30-059, Poland

[2] Institute of Technical Sciences and Aviation, The University College of Applied Sciences in Chełm, ul. Pocztowa 54, Chełm 22–100, Poland

* Corresponding author's e-mail: plonkwic@panschelm.edu.pl

ABSTRACT

The working surface of lift guide rails during operation is exposed to the destructive action of catchers under emergency braking conditions. In most cases, this surface is lubricated with grease, which makes it impossible to visually assess their local wear. The comfort of cabin movement on guide rails and thus the feelings of cabin occupants depend on the condition of guide rails. Therefore, the verification of lift guide rails wear under real conditions (in situ) is quite cumbersome. In order to assess them on a monthly basis, they would have to be completely cleaned and the excessively worn areas would have to be measured with universal measuring tools and re-lubricated. Such activities would only be a waste of time and lubricant. Therefore, the concept of a magnetic head was developed to assess the technical condition of lift guide rails. The head, which uses permanent magnets, makes it possible to measure the dispersed magnetic field of the guide rail cross-section. The areas of excessive wear show changes in this field, so it is possible to identify these areas without a need to remove lubricant from their surface. This paper presents both the detailed design of a developed head and the preliminary results of measurements using it. As the lift guide rails can have different dimensions depending on the lifting capacity, the developed head was equipped with inserts having the dimensions compatible with the guiding part width, thus enabling measurements that can be taken on different types of guide rails. The developed head and methodology allow measurements to be made without the need for disassembly, i.e. under in situ conditions. The results obtained in the laboratory have shown that the head concept and the measurement methodology are suitable for measurements in situ and perfectly fill the gap in this field of mechanical engineering.

Keywords: guide rail, non-destructive testing, lifts, safety, reliability, magnetic field.

INTRODUCTION

Non-destructive testing was described in the literature by many authors and with reference to various fields. Also, the rope-related issues were described in the literature.

In the article [1], the authors described the design of their own concept of a magnetic head which they used for the diagnosis of hybrid ropes, i.e.: steel ropes in polyurethane matrix. Such ropes have that their metal core potted in plastic, which makes them very difficult to diagnose. Wire strand breaks and local narrowing affect not only safety, but also durability. The head design and diagnostic methodology proposed by the authors provide a qualitative and quantitative assessment of the technical condition of hybrid ropes. In the publication [2], the authors described the use of numerical analyses of magnetic field distributions for qualitative assessment of the lift guide rail wear. The main purpose was to demonstrate the possibility of using the permanent magnetic field and the scattering field to effectively locate the places of damage in steel guide rails, as

well as to verify the possibility of conducting the quantitative assessment related to the evaluation of a degree of wear of guide rails with regard to the service life of passenger lifts. The method itself received patent protection in the Republic of Poland and the first prize during the competition organised by Elevator World in the Project of Year 2020. In the publication [3], the authors presented the results of laboratory tests in which they used their own concept of a magnetic head for the assessment of technical condition of lift guide rails. Since it is quite difficult to assess the technical condition of guide rails under operating conditions, the proposed method was validated on a laboratory bench and its results gave positive results. In the article [4], the authors presented the results of own research on the use of measurements of magnetic field and analysis of its variability to detect damage and wear of cables in belt conveyors. In the considerations made, the authors proposed the data preprocessing technique developed to synchronise signals for data with oblique convolution. Since the quality of convolution is related to its corresponding precision, they defined the convolution evaluation as the analysis of each signal similarity to an estimated pattern. Furthermore, the authors proposed an automated procedure applied to real measurement data and final results. In the article [5], the authors presented the results of their own research during which they applied non-destructive testing to assess the condition and age of aircraft landing gear components. The tests were carried out in accordance with the applicable legal regulations and standards. In the article [6], the authors described the use of computed tomography to assess the surfaced layer hardness. In the first part of the article, the authors described the defects obtained in relation to the influence and type of wire. Based on the obtained results and photographs, they determined the basic mechanical properties of the deposited coatings. In the article [8], the authors presented a broad overview of static and dynamic studies published on SHM and NDT of slender masonry structures, summarising and discussing various experimental techniques used in relation to dynamic testing. According to the authors' analysis, the technique being most commonly used by the researchers is the Operational Modal Analysis (OMA) using accelerometers, but other promising methods such as radar interferometry are also described. The paper is concluded with a brief review containing the examples of numerical assessment of the structure condition and the signal processing tools. It also presents a list of papers describing the most important features of slender masonry structures, natural frequencies, experimental and numerical techniques used and reference values.

In the publication [9], the author presented the magnetic flux leakage (MFL) as the basis for an automated wire rope condition monitoring system in which the human factor was completely eliminated. The author developed his own research results based on the use of ropes from various industries, which are described in detail in EN standards – in the case of ropes used in cableways, and in IMCA standards – concerning ropes used in the marine industry. The research was conducted using the ropes of loading cranes, mining winches, cableways, cable-stayed bridges, pillar chimneys, antenna masts, overhead transmission lines and other installations. In the article [10], the authors presented the results of their own research on the NDT method application for the assessment of ropes used in cranes. The authors focused their attention on the application of this method to assess the internal condition of ropes. They compared the obtained results to the ISO 4309 standard recommendations. In the publication [11], the authors presented an overview of the most common defects found in additively manufactured components as well as various NDT assessment methods applicable to additively manufactured components and their ability to detect and control defects that occurred during component manufacture and handling. They also discussed the suitability and challenges related with the non-destructive technique application to various additive manufacturing processes and parts.

This article presents the results of own research on the evaluation of lift guide rail wear due to contact with structural elements of catchers operating under emergency braking conditions. The case under consideration results in the guide rail surface becoming plastically deformed (damaged), and the research aim was to identify these damages and their qualitative assessment with respect to further operation.

TEST OBJECT DESCRIPTION

Passenger lifts are machines whose trajectory is determined by steel guide rails positioned opposite one another, as shown in Figure 1.

During normal use of lifts, their stopping is induced by the pressure of suspension cables on the friction wheel located on the drive unit. This pressure is so great that stopping the car at any place does not cause any deformation on the guide rails because, in this case, the brakes do not interact with the guide rails.

The case of the interaction of brakes with guide rails is the so-called emergency braking situation. This case occurs when the lift car exceeds the nominal speed by 0.3 m/s, whereas the reasons for exceeding the speed may be as follows [15]:

- failure of the drive unit, causing the friction wheel to rotate at a higher speed,
- breaking of all load-bearing straps,
- failure of the control unit, causing an increase in rotational speed of the friction wheel.

While the above causes can be classified as operational ones, the uncontrolled application of brakes may also be due to installation factors, i.e. incorrect adjustment of brakes in relation to the guide rail surface. In this case, during normal drive of the car at nominal speed, the brakes can be activated which, when engaged, will plastically deform the guide rail surface through its contact with the braking elements (roller and stop plate) of the catcher.

The object of laboratory tests was a steel guide rail with a T-section, the geometry of which is shown in Figure 2.

Table 1a summarises the main geometric and 1b strength parameters of the S275B material from which the RP 90/B lift guide rails are manufactured, and Figure 3 shows the main geometric designations [12].

It is worth noting that the S surface (Figure 2) of the guide rail as a new one has a tolerance of 0 to +0.1, which means that the maximum width of the new guide rail is 16.1 mm. Therefore, this value decreases fairly uniformly over its entire length during the normal use of the lift. Its wear under normal operating conditions, i.e. without contact with the catcher roller, does not lead to concentration of metallic particles in the lubricant as the mating guides have the inserts made of plastic.

Only emergency braking causes local deformation, the size of which depends on a number of factors, and the deformation itself is removed mechanically (by manual cleaning with a grinder) causing local reduction of the guide rail width, i.e. dimension k, which influences the size of contact between the braking elements of the catcher with the guide rail.

In order to identify such places and their size along over the entire length of the guide rail, a prototype head was developed that would allow such identification by means of a dispersed magnetic field. The research object was a guide rail on which a deformation area A was simulated in laboratory conditions, caused by emergency braking, and then cleaned in the same way as under real conditions, shown as deformation B. Then this area was analysed using the developed head in order to assess it.

The laboratory tests were carried out on the basis of the hypothesis that it is possible to identify faults on the guide rail's surface using dispersed magnetic field.

The design assumptions of the head and the way it works were reported as a utility model to

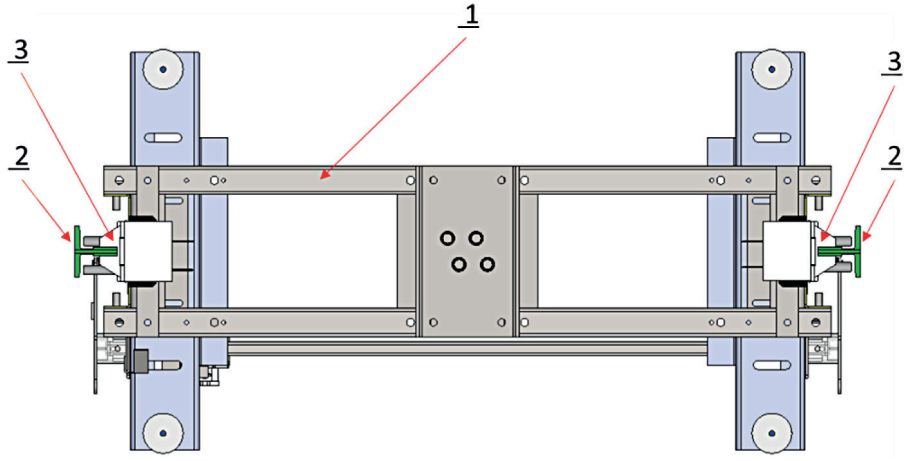

Figure 1. Position of guide rails in relation to passenger lift support frame:
1 – support frame, 2 – guide rail, 3 – sliding guide rail

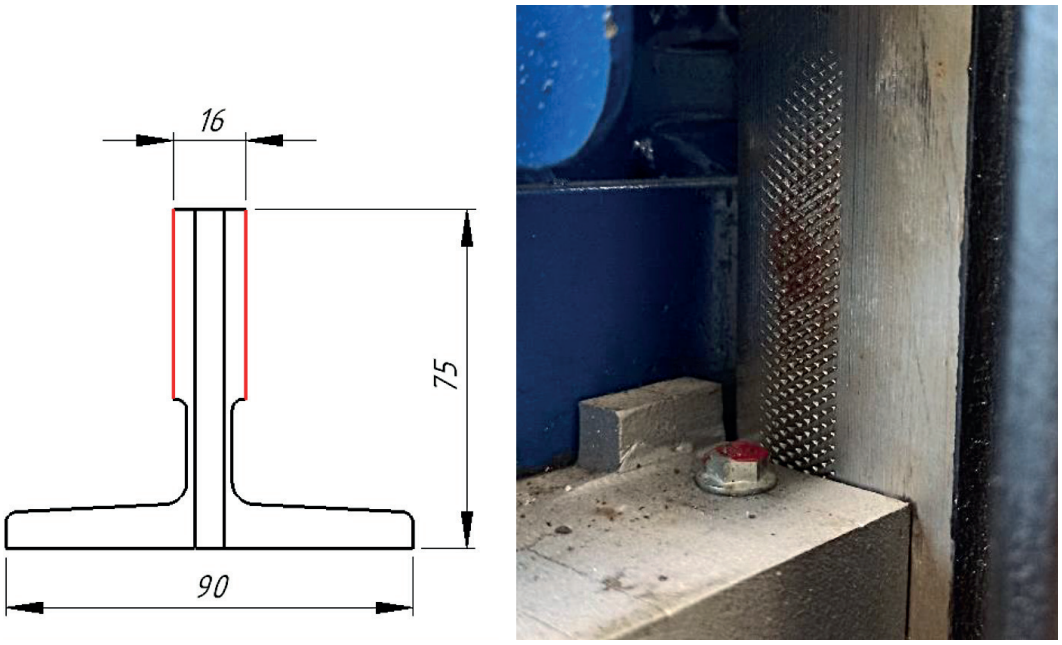

Figure 2. View of RP90/B guide rail with main dimensions and red-marked working surface S, plastic deformed guide rail surface after engaging the catcher.

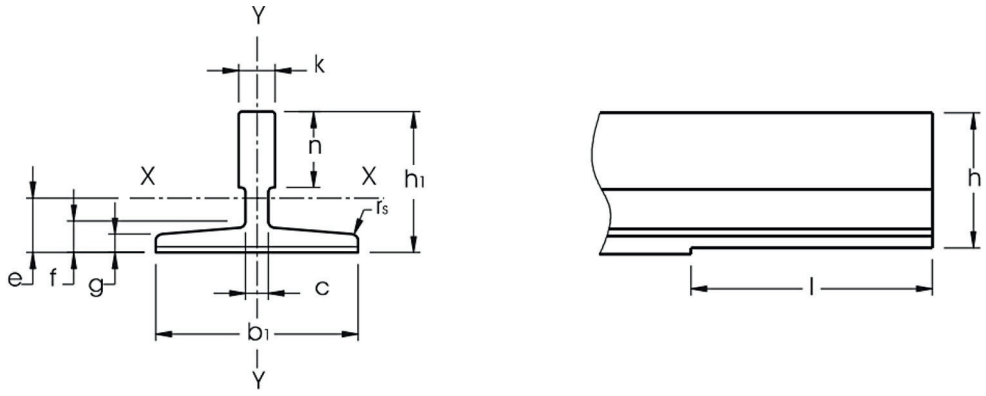

Figure 3. Main geometrical designations of RP90/B-type guide rail [12]

Table 1. Geometrical and strength parameters of material S275B [12]

a							
b_1 [mm]	h_1 [mm]	h [mm]	k + 0,1/0 [mm]	n [mm]	c [mm]	g [mm]	f [mm]
90	75	74	16	33.4	10	7.9	11.1
b							
S [cm^2]	q_1 [kg/m]	I_{xx} [cm^4]	W_{xx} [cm^3]	I_{yy} [cm^4]	W_{yy} [cm^3]	e [cm]	
17.25	13.55	102	20.87	52.6	11.8	2.61	

the Polish Patent Office under No. Ru072199m while the concept of the diagnostic head for the technical condition assessment of the lift guide rails and the measurement methodology were appreciated at the ELEVATOR WORLD's 2020 Project of the Year, obtaining the first prize in the category of Elevators – Upgrades and Repairs.

MEASURING HEAD CHARACTERISTICS

Based on the adopted hypothesis and the selected design assumptions described in the utility model protected by industrial property rights, a numerical experiment was carried out, as described in detail by the authors in the article [2].

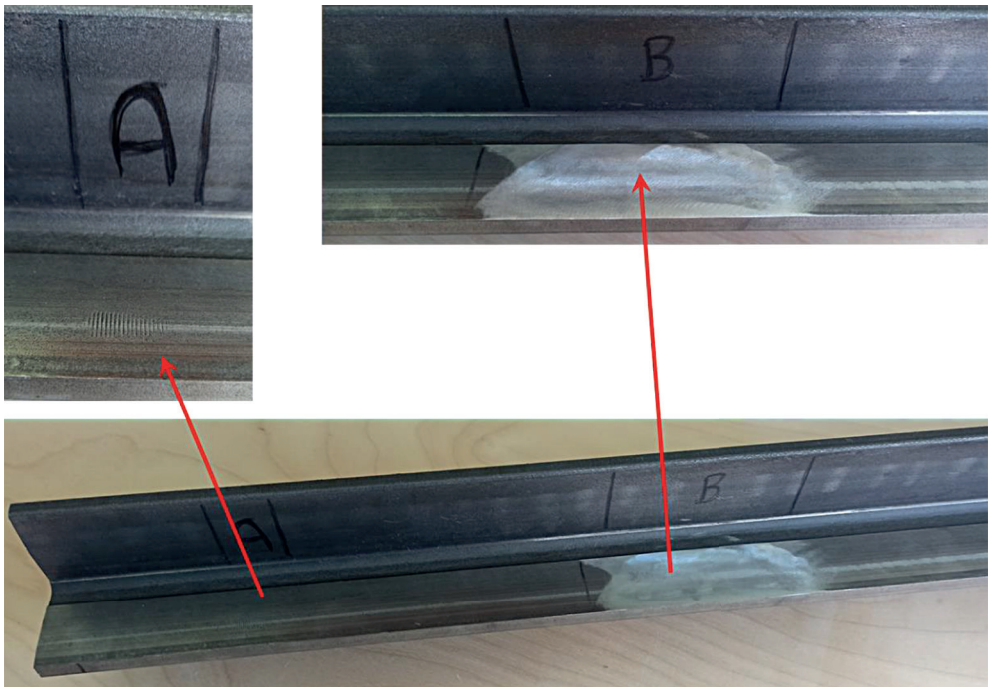

Figure 4. Plastic deformation area made to validate the measurement path: A – trace caused by the catcher brake roller, B – cleaned area after the trace caused by the catcher brake roller

The authors developed a CAD model consisting of a guide rail with a local defect and the magnetic circuit of the measuring head. Using the experience of designing and constructing magnetic circuits for wire rope diagnostic heads with the use of numerical analyses concerning multi-criteria optimisation [1, 2, 3], the initial shapes and dimensions of the magnetic core elements were adopted and NdFeB-N52 permanent magnets with suitably high magnetic energy were selected. Upon analysing numerically (Fig. 5) the magnetic field distributions in the magnetic core and the guide rail tested, the defect dimensions such as defect width (sz = 50–150 mm) and defect depth (g = 0.3–2.0 mm) were assumed as variables. These dimensions correspond to the actual losses in the guide rail cross-section after mechanical levelling in the deformation area after operation of brakes (catchers).

The numerical analyses confirmed the adopted hypothesis and allowed to determine the dimensional parameters of the magnetic circuit,

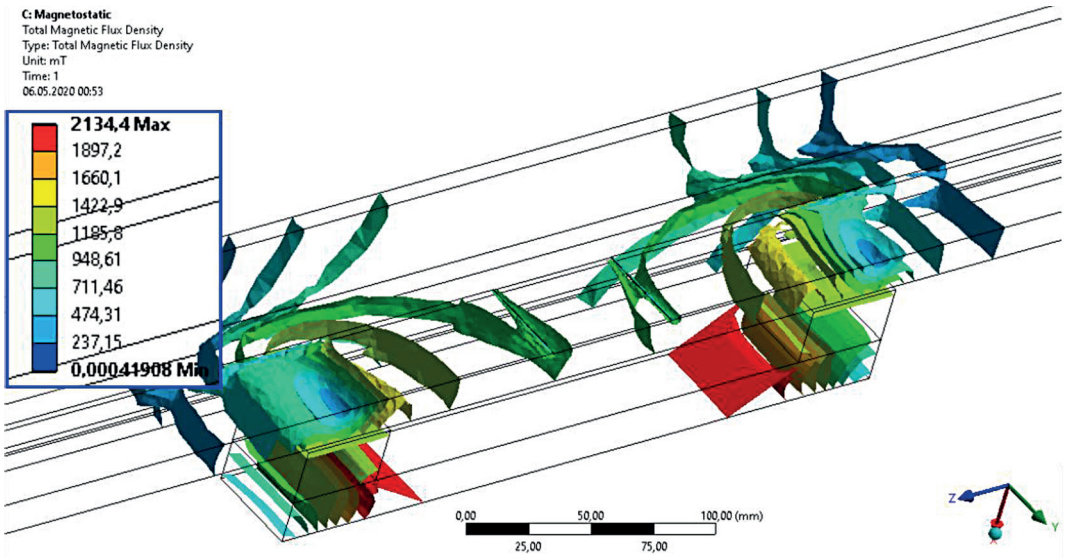

Figure 5. Distribution of magnetic field induction in the guide rail and magnetic circuit of the head

i.e. jumper dimensions of 245×60×19 mm and magnet dimensions of 50×50×13 mm, which ensure adequate metrological parameters. The correctly determined geometrical and material parameters of the magnetic circuit guarantee the appropriately high value of magnetic induction B of about 1000 mT in the guide rail and the magnetic dispersion field in the areas where defects occur. It has been proved that for the adopted design parameters of the magnetic core and the assumed parameter variation level characterising the defect size (cross-section loss), it is possible to achieve a measurable level of magnetic induction change in the area of defect occurrence.

The numerical analyses showed that the magnetic field induction variation caused by a defect would occur in the magnetic field component in line with the guide rail direction and in the component perpendicular to the deforming surface, which was confirmed by the results from the laboratory measurements described in the further part of this paper.

Based on the determined parameters of the magnetic circuit, a complete 3D CAD structural model of the measuring head was developed using the SolidWorks software. Due to the prototype nature of the head and the need for its validation due to the prototype nature of the measuring head and the need for its validation in laboratory conditions, it was assumed that some elements would be made in the 3D printing technology, which shortened the time and reduced the costs of prototype manufacturing and fulfilled the requirements for non-magnetic properties of the remaining structural elements, apart from the magnetic core. The head model (Fig. 5 and 6) consists mainly of the body (1), which is at the same time the supporting and assembling element for the remaining components, as well as the guiding element due to the contact of surfaces marked as A and B (Fig. 7) with the surfaces of the head guide rail when moving the head along the guide rail. The body (1) is provided with a socket of the rotary encoder (2) on the shaft of which a rotary disc in contact with the guide rail is installed (Figure 7). The encoder acts as a path converter indicating the defect location along the guide rail length. The encoder seat is fixed on the rotary axis, which enables adjustment of its position depending on the guide rail head thickness – "k" parameter (Fig. 3). In the physically-made head, the encoder seat (2) is tensioned towards the body (1) and the guide rail by means of a spring (Fig. 9). Two oppositely polarised permanent magnets (3) seated in the body (1) and fixed with caps (6) are the source of magnetic field. The magnetic circuit is closed by a jumper (5). In Figure 7, both the jumper (5) and the magnets (3) are shown symbolically with their real dimensions omitted so as to make the illustration and the description of the diagnostic head structure clear.

The magnetic jumper does not require any fixing elements due to the cohesion (attractive) forces from permanent magnets. Considering the measurement and the universal point of view, the most important element is the sensor displacement system (4) which allows the adjustment of the sensor position both in the direction of plane

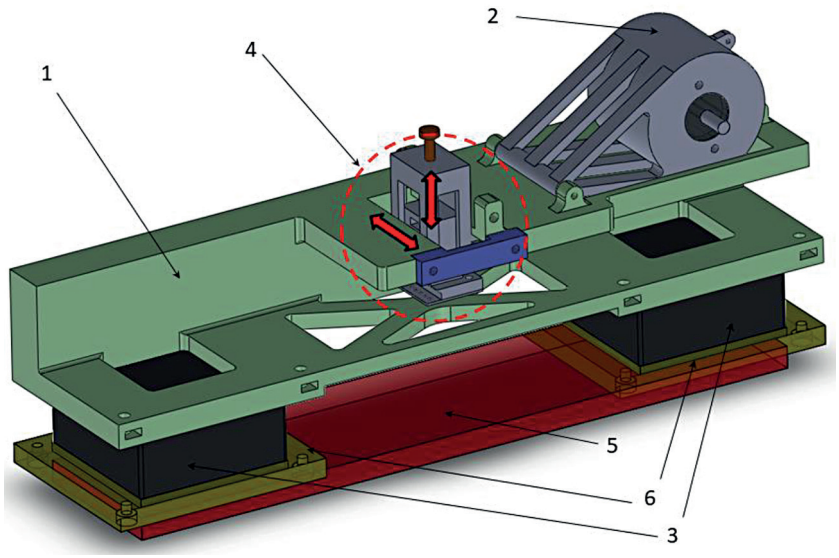

Figure 6. 3d CAD model of the measuring head (isometric view)

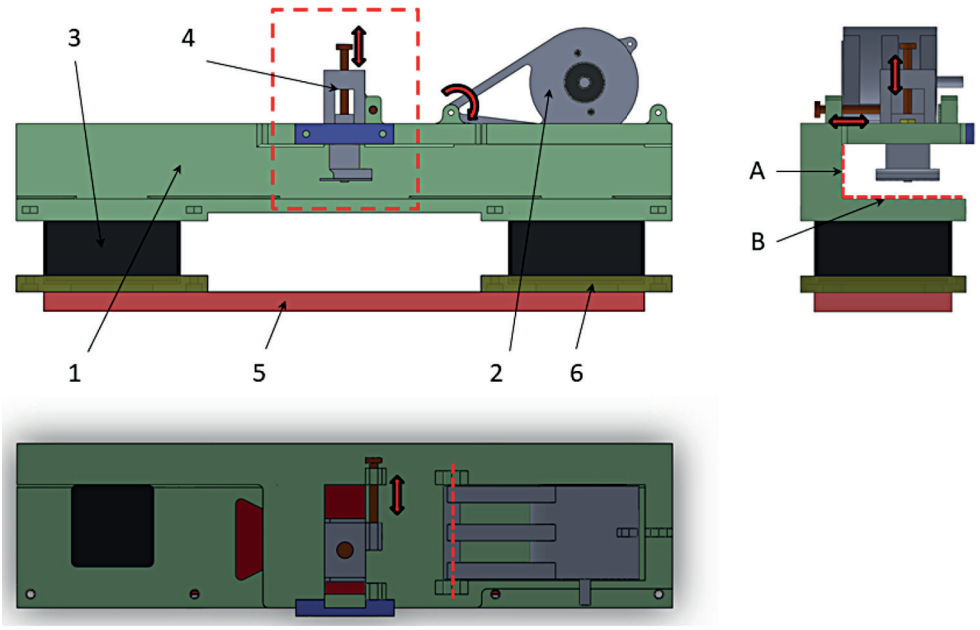

Figure 7. 3d CAD model of the measuring head (orthographic projection)

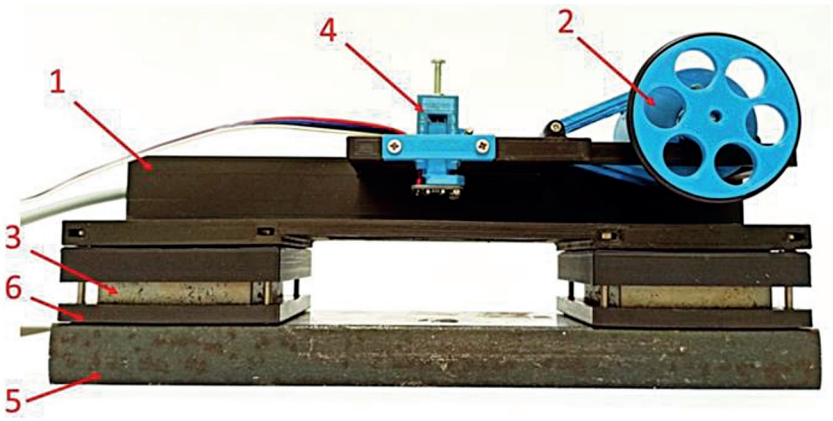

Figure 8. Measuring head made in the FDM printing technology armed with magnetic core and sensor elements (magnetometer and encoder): (1 – body; 2 – encoder, 3 – permanent magnets, 4 – sensor displacement system, 5 – jumper, 6 – caps)

A and plane B (Fig. 7) depending on the guide rail head geometry and dimensions.

As it was necessary to make the main structural components of non-magnetic materials, they were made on the basis of CAD model using Fused Deposition Modelling (FDM) 3D printing technology. As the head is not mechanically loaded in any way, the Polyactide (PLA) material was used for its manufacture, while fasteners were made of stainless materials. Figure 8 presents the prototype measuring head used for laboratory tests, armed with a magnetic circuit and sensory elements related to the dispersed field measurement and the defect location.

Figure 9 presents a prototype head installed on a lift guide rail prepared for laboratory testing. This is the first version of the prototype which, based on observations from laboratory tests, will be improved in terms of functionality, metrology and data acquisition during further research and development works.

The measurement system (Figure 10) consisted of a module for recording the dispersed magnetic field, which was built based on the 3-axis digital magnetometer MLX90393 (1) and the ArduinoMega (2) microcontroller, and the displacement recording module which consisted of the incremental encoder Eltra ER30 (3) and the measurement card NI USB-6216 (4). The whole system was powered by the laboratory power supply Zhaoxin RPS-3005DB 30V 5A (5). Acquisition of the recorded signals was performed

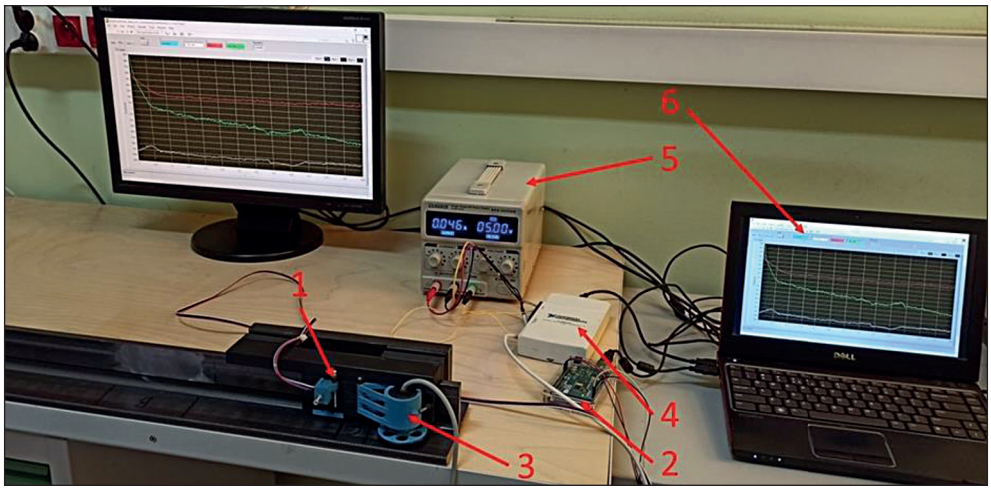

Figure 9. Measuring head installed on a guide rail under laboratory conditions: (1 – body; 2 – encoder, 3 – permanent magnets, 4 – sensor displacement system, 5 – jumper, 6 – caps)

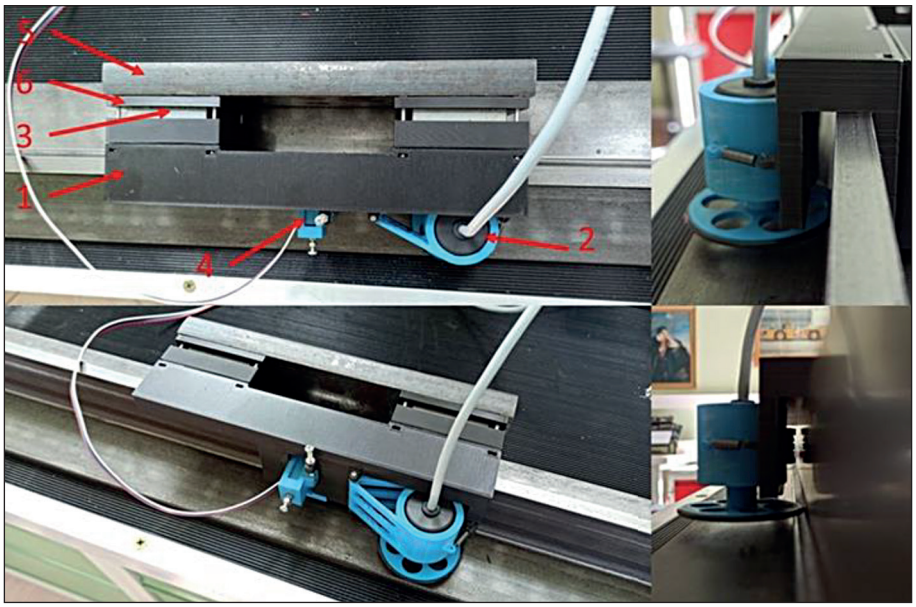

Figure 10. Diagnostic measurements of a guide rail under laboratory conditions

using a program developed for this purpose in the LabView environment (6).

RESULS

Tests with the use of developed prototype measuring head were carried out on the lift guide rail of RP90/B type in the area with the continuous damage (area B – Fig. 11) in the form of its grinding in the place of catcher operation.

During the research, 15 series of measurements were carried out, of 3 magnetic field induction components (B_x, B_y, B_z). The measuring system was moved along the distance of 0.5 m and the magnetic sensor was located at a distance of a=1mm from the side surface and b=18mm from the guide rail head; its position and orientation in relation to the guide rail under test is shown in Figure 11. The measuring head was moved manually, while the use of a Hall-effect sensor eliminated the influence of speed variation on the recorded magnetic field induction values. The sampling frequency of the measuring system was 50 [Hz] and the distance between successive measuring points along the tested guide rail length did not exceed 0.6 [mm]. Based on the tests recorded, a standard uncertainty analysis was carried out, using the A method (method of calculating uncertainty by statistical analysis of a series of single observations). The A method can be used in measurements where a random error is present. The

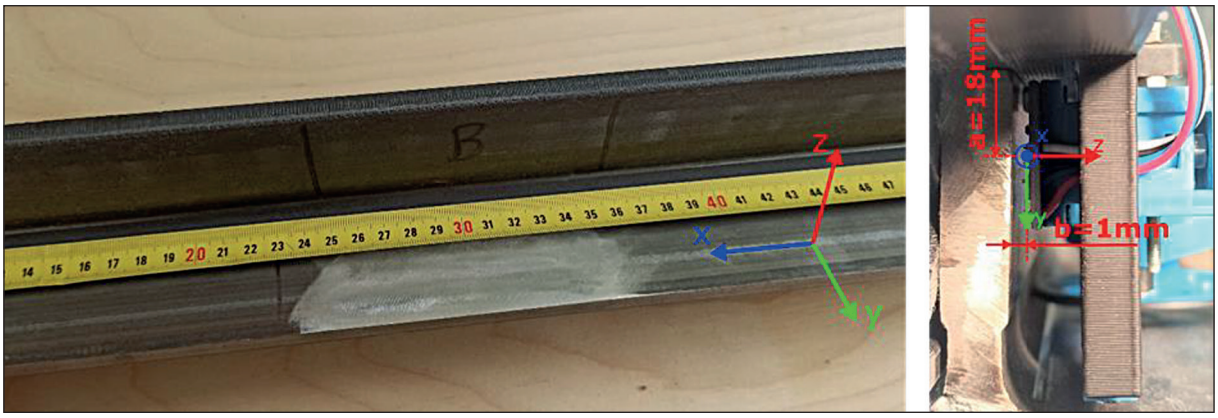

Figure 11. Position and orientation of a measuring sensor over the guide rail under test

simplest case is the analysis of a series of n observations q_1,...,q_i,...,q_k. Individual q_k observations (magnetic induction measurements) vary in value due to random changes in input quantities or random interactions. The quantity characterizing the variation of observed q_k values, their scatter around the mean $\overline{q}$, is the $s(q_k)$ experimental standard deviation expressed by the relation (1). The $s(q_k)$ value could be identified with the measurement uncertainty if any of the q_k values were taken as its result [13, 14].

$$s(q_k) = \sqrt{\frac{\sum_{k=1}^{n}(q_k - \overline{q})^2}{n-1}} \qquad (1)$$

Based on the recorded signals, the average values of magnetic induction components $s(B_x)$; $s(B_y)$; $s(B_z)$ were determined as well as their $s(B_x)$; $s(B_y)$; $s(B_z)$ experimental standard deviations determined from the relation (1). The obtained results are presented in Figure 12.

The recorded change in the values of B_x, B_z components of magnetic induction occurring in the area of the modelled damage was shown in the region of approximately 0.25–0.35 m. The presented results are repeatable, which is evidenced by small changes in experimental standard deviations.

The highest uncertainty is found in the results recorded for the B_z magnetic induction component with an average value of 11.8% relative standard deviation along the length of the area under test. For the x and y components, this value does not exceed 5%.

Figure 13 presents the values of B_x, B_z components of magnetic induction recorded during one of the measurements. The presented signal was

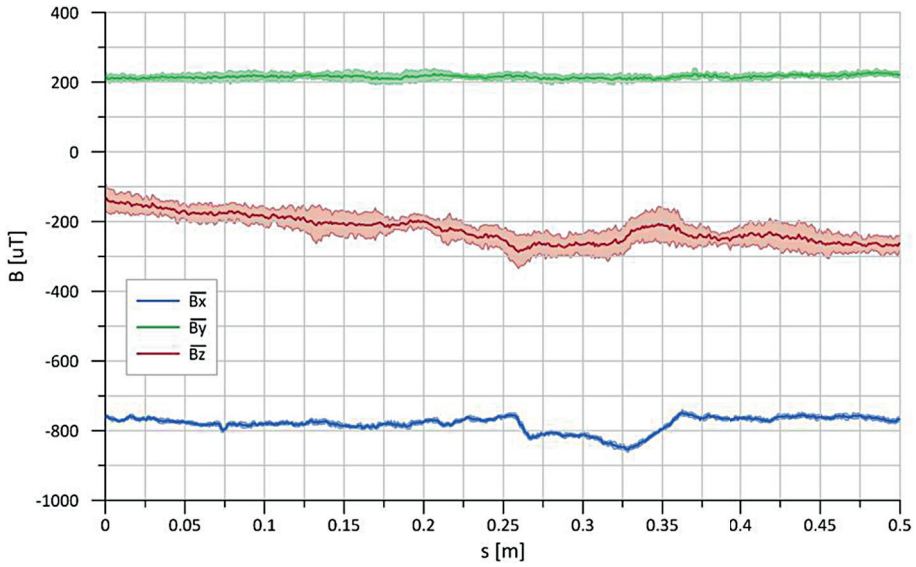

Figure 12. Mean values of magnetic induction components ($\overline{Bx}$; $\overline{By}$; $\overline{Bz}$) and their experimental standard deviations s(Bx); s(By); s(Bz)

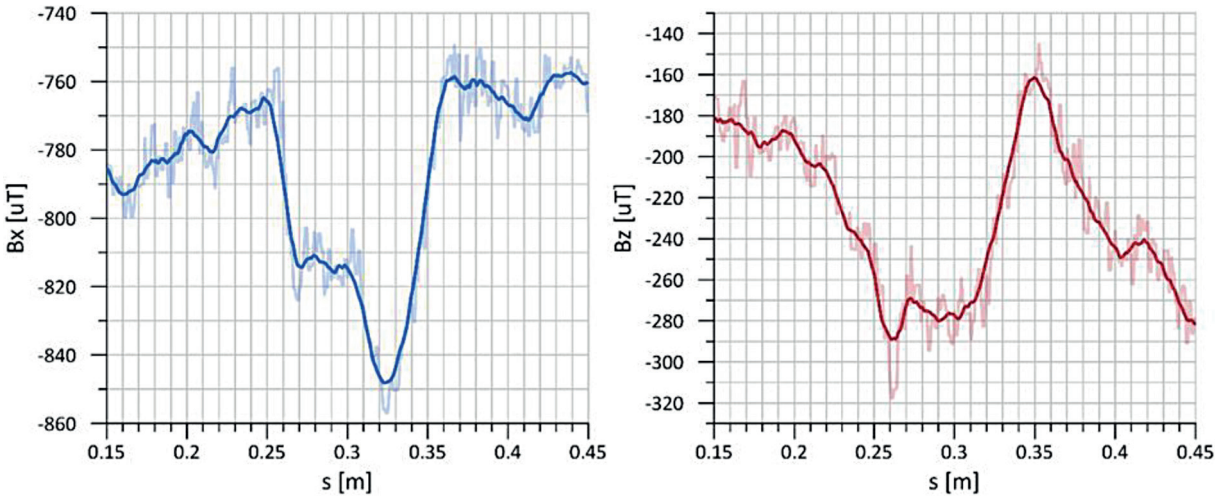

Figure 13. Recorded values of Bx, Bz magnetic induction components

limited to the interval of 0.15–0.45 m; due to the lack of diagnostic information, in the further part of the analysis the B_y component was omitted.

In order to increase the possibility of identifying the damage location, the gradient of the recorded signal B_x, B_z was determined (Figure 14). In places corresponding to the beginning and end of the damage, a clear change of values of determined gradients is visible.

In order to better visualise the damage location, the product of the previously calculated B_x, B_z gradients was determined (Fig. 15). These calculations enabled to obtain a relationship that unambiguously makes the damage identification possible. The characteristic feature of the extreme areas of damage is a clear change in the gradient product value of the B_x and B_z components, while in other areas this value oscillates around zero. Figure 15 shows the determined product of signal gradients and the results of damage depth measurements which were carried out using the Profilometr Formtracer Mitutoyo Svc450 profile gauge. The tests were carried out in such a way that the measuring line of the profile gauge coincides with the measuring line of the magnetic sensor (a = 18 mm, b = 1 mm – Fig.11).

CONCLUSIONS

The laboratory tests and observations proved metrological effectiveness of the adopted method and validated the developed prototype functionality in laboratory conditions. At the same time, the conclusions from previously conducted numerical tests described in the article [2] were confirmed and the hypothesis was proven. Moreover, an important aspect of the

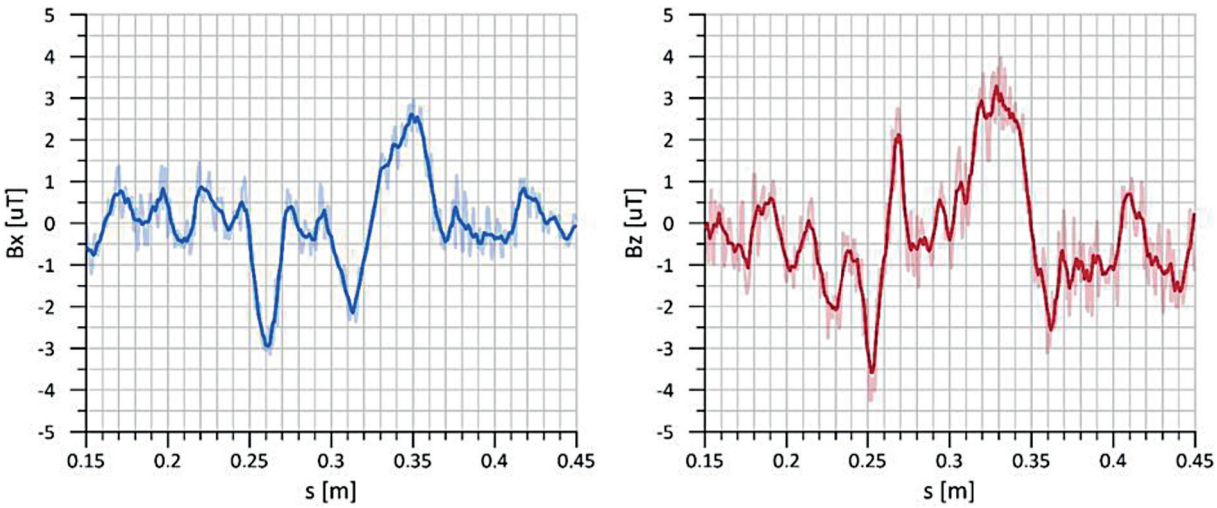

Figure 14. Gradient of recorded value of Bx, Bz magnetic induction components

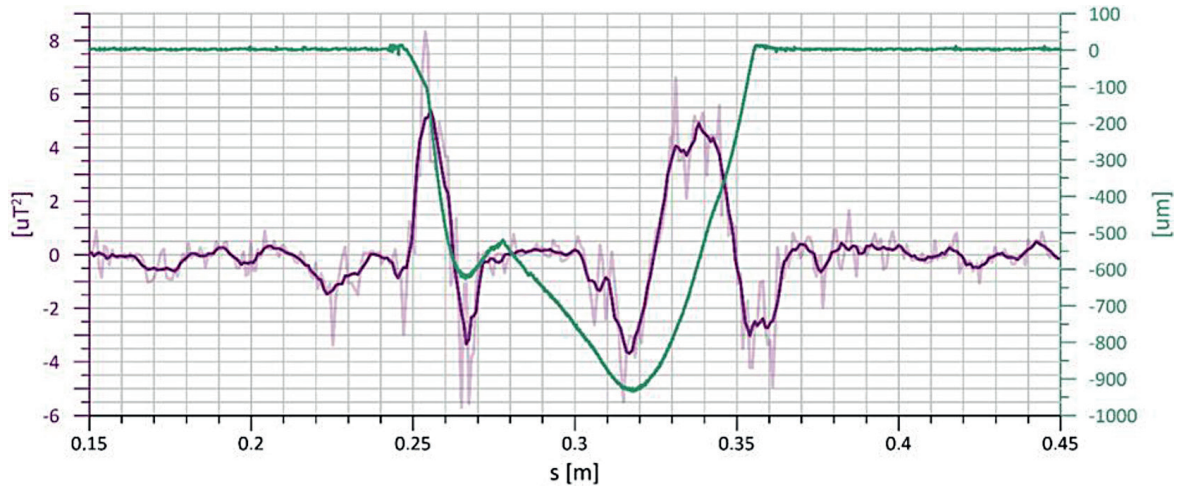

Figure 15. Product of gradients of recorded Bx, Bz magnetic induction component values and results of measurement made with profile gauge

conducted research is that the proposed methodology and measurement method is a pioneering solution and the guide rails were not submitted to any other tests to determine their technical condition.

The activities described in this paper have revealed the areas of the presented prototype design that need to be improved, mainly in the following scope: increase of the structure rigidity and strength during the construction of a next prototype for in situ validation and commercial applications; replacement of the frictional guidance of the head along the guide rail by the rolling guidance; stabilisation of the guidance to eliminate the head and sensor vibration in relation to the guide rail under test; introduction of improvements in the distance transducer so that the encoder disc does not slip in case of lubricants on the guide rail; adaptation and improvement of the data acquisition system to work on the real object; testing of the magnetic field sensors of different designs and with higher sensitivity; performance of more quantitative comparative tests on the damage standards to compare the methodology adopted to the existing approach; development of the limit state indication systems for a given geometrical and dimensional type of guide rail and an accepted level of loss.

The above presented proposals for changes in design and metrology should improve the working culture of the device and result in a greater sensitivity of measurements, repeatability of results and precision of quantitative evaluation.

REFERENCES

1. Ruta H., Krakowski T., Lonkwic P. Optimisation of the magnetic circuit of a measuring head for diagnostics of steel-polyurethane load-carrying belts using numerical methods. Sustainability. 2022; 14(5): 1–19.
2. Lonkwic P., Krakowski T., Ruta H. Application of stray magnetic field for monitoring the wear degree in steel components of the lift guide rail system. Metals. 2020; 10(8): 1–19.
3. Lonkwic P., Krakowski T., Ruta H. Assessment of the technical condition of lift guide rails using a magnetic field. VI International Conference of Computational Methods in Engineering Science (CMES 2021). Poland 2020, 9–10.
4. Kozłowski T., Wodecki J., Zimróz R., Błażej R., Harygóra M. A Diagnostics of conveyor belt splices. Applied Sciences. 2020, 10(18).
5. Malec M., Cieplak T., Walczuk S. Non-destructive tests of lock tongues used in ATR-72 aircraft landing gear based on magnetic method. Adv. Sci. Technol. Res. J. 2013; 7(20): 23–28. https://doi.org/10.5604/20804075.1073049
6. Józwik J., Dziedzic K., Usydus I., Ostrowski D., Korolczyk G. Assessment of internal defects of hardfacing coatings in regeneration of machine parts. J. Cent. South Univ. 2018, 25: 1144−1153.
7. Sadowski Ł., Stefaniuk D., Różańska M., Usydus I., Szymanowski J. The effect of waste mineral powders on the structure of air voids in low-strength air-entrained concrete floor screeds. Waste and Biomass Valorization. 2020; 11: 2211–2225.
8. Pallarés F., Betti M., Bartoli G., Pallarés L. Structural health monitoring (SHM) and nondestructive testing (NDT) of slender masonry structures: A

practical review. Construction and Building Materials. 2021; 297

9. Vasily V., Sukhorukov V. Steel Rope Diagnostics by Magnetic NDT: From Defect Detection to Automated Condition Monitoring. Materials Evaluation. 2021; 79(8).
10. Peterka P., Krešák J., Vojtko M. Experience of the Crane Steel Wire Ropes Non-Destructive Tests. Adv. Sci. Technol. Res. J. 2018; 12(4): 157–163. https://doi.org/10.12913/22998624/100350
11. Sreeraj P.R., Mishra S.K., Singh P.K. A review on non-destructive evaluation and characterization of additively manufactured components. Progress in Additive Manufacturing. 2021; 7(2): 225–248. https://doi.org/10.1007/s40964-021-00227-w
12. http://www.monteferro.it/wpcontent/uploads/2020/05/Monteferro_Standard_Machined_Guide rails.pdf
13. Zięba A. Physical Laboratory of the Department of Physics and Nuclear Technology of AGH University of Science and Technology, Part I. Pracownia Fizyczna Wydziału Fizyki i Techniki Jądrowej AGH, Część I. Wydanie trzecie zmienione. Publisher AGH Kraków, 2002.
14. JCGM 100:2008 Évaluation des données de mesure – Guide rail pour l'expression de l'incertitude de mesure.
15. Polish Standard PN EN 81.20, Safety Regulations Concerning the Structure and Installation of Lifts. Electric Lifts.